Penerbit Akademia Baru

Journal of Advanced Research in Fluid Mechanics and Thermal Sciences
ISSN (online): 2289-7879 | Vol. 25, No. 1. Pages 1-18, 2016

The Significant Effect of Secondary Flow in Wavy Microchannel for Augmentation of Heat Transfer

I. A. Ghani

Faculty of Mechanical Engineering, Universiti Teknologi Malaysia, 81310 Skudai, Johor Bahru, Johor, Malaysia.
iaghani68@yahoo.com

Abstract - *The heat transfer augmentation methods have received a great attention from many researchers to enhance heat transfer in conventional thermal applications. Recently, many studies have adopted passive methods to enhance heat transfer in microchannel heat sink. Channel curvature and secondary flow are two of the methods in which their effectiveness in this field have been proven. In the present study, a combination of these two methods was applied to enhance heat transfer rather than using individual method. Three-dimensional numerical analysis of conjugate heat transfer was conducted in a wavy microchannel with oblique secondary channel in alternating orientation (WAOC). The study presented the effects of three structural parameters on hydrothermal performance with the amplitude ranged from 0.05 mm to 0.2 mm, a secondary channel width between 0.1 mm and 0.2 mm, and an angle of inclination between 45° and 90°. The results were compared with wavy microchannel without secondary channel (WWOC) and also with straight microchannel of the same cross-section. The thermal performance of WAOC increased for about 108% with optimal structural parameters of 0.1 mm amplitude, 0.2 mm secondary width, and 45° angle of inclination. The results also revealed that the Nusselt number of WWOC increased for about 28.5% more than WWOC.*

Keywords: wavy channel, secondary flow, micro-channel heat sink, laminar flow

1.0 INTRODUCTION

The rapid development of electronic industry, particularly in the field of integrated circuits (IC), resulted in the emergence of new generations of high-performance processors in terms of speed and capacity. These processors require more power consumption, and thus more heat is generated within it. According to the International Technology Roadmap for Semiconductor (ITRS), the peak power consumption for lower-end desktops will rise up to 95% (91w-158w) and 96% (147w-288w) for high-performance desktops in 2016 [1]. In other words, the conventional cooling devices such as fins and fans have become inadequate to meet the ever-increasing cooling requirements. Therefore, it has become imperative to find an effective cooling method as an alternative to conventional methods. One of the promising solutions to this problem is direct liquid cooling incorporating microchannel. It is one of the alternatives which has been used widely for cooling tiny electronic components due to the favorable and attractive features such as light weight, compactness, and higher heat transfer area to volume ratio. Tuckerman and Pease [2] have proposed the first concept of microchannel heat sink (MCHS) by experimental study. The study was conducted by exposing the substrate of a silicon

MCHS to a heat flux. The result proved that the proposed MCHS can remove a heat flux of 7.9×10^5 w/m^2 with a maximum temperature difference of 71 °C between the substrate and the inlet water. Although the results represent a significant achievement in the field of electronic cooling methods, especially for high power density application, the shortcoming of this method lies in the high-pressure drop across the microchannel. This increment in pressure drop leads to increase the pumping power consumption.

Therefore, a lot of experimental and numerical studies have been conducted which aim to enhance the hydrothermal performance of microchannel through various methods. Initial studies have been focusing on improving the performance by manipulating the geometric parameters of microchannel such as height, width, and aspect ratio to obtain optimal results of maximum heat transfer rate with a minimum pressure drop [3-5]. Lee et al. [6] have conducted an experimental study of single-phase heat transfer through rectangular microchannel for a wide range of hydraulic diameters (318 µm - 903 µm). The study aimed to detect the correlations validity of conventional sized channel in the prediction of thermal behavior in a rectangular microchannel. The results showed the possibility of employing conventional analysis approach in the prediction of heat transfer analysis in microchannel. Other researchers have focused on the influence of cross-section shape by studying various shapes such as circular, triangular, and trapezoidal [7-12]. Alfaryjat et al. [13] have studied numerically the influence of geometrical parameters on the thermal performance of various cross-section channel shapes. The study covered three shapes; hexagonal, circular, and rhombus. The results showed that hexagonal cross-section MCHS had the highest pressure drop and heat transfer coefficient. Also, the highest value of friction factor and thermal resistance were found with the use of rhombus cross-section MCHS. In a separate study, Gunnasegaran et al.[14] have carried out a numerical simulation to study the effect of geometrical parameters namely rectangular, trapezoidal, and triangle MCHS on thermofluid performance. The results showed that the highest heat transfer enhancement was found in rectangular MCHS followed by trapezoidal and triangular MCHS.

Steinke and Kandlikar [15] have reviewed single-phase heat transfer enhancement techniques. The study focused on the possibility of applying these techniques in microchannels. Several passive techniques have been specified in which they can be applied in microchannels such as flow disruptions, channel curvature, re-entrant obstructions, secondary flows, and fluid additives. In the recent years, many researchers have adopted these techniques to enhance the thermal performance of a microchannel. Channel curvature is one of the techniques that has attracts the attention of many researchers. Sui and co-workers [16] have submitted a series of studies which investigated the heat transfer in a wavy microchannel. they studied numerically the heat transfer and fluid flow in wavy microchannel with rectangular cross-section under constant wall temperature (T), constant heat flux (H2), and conjugate conditions. The study revealed that a significant enhancement in heat transfer had been achieved as a result of Dean vortices which was generated when the coolant flowed through the wavy channel. These vortices enhance the folding and stretching of the flow element which in turn increase the chaotic mixing. In another study by Sui et al [16], they investigated experimentally the flow and heat transfer in sinusoidal microchannels with rectangular cross-sections. Each microchannel consisted of ten wavy units with a depth of 404 µm, an average width of 205µm, a wavy amplitude between 0 µm - 259 µm, and a wavelength of 2.5mm. Deionized water was used as the working fluid with a range of Reynolds number from 300 to 800. The results showed that the heat transfer performance of the wavy microchannels was much better than that of straight microchannel. At the same time, it was also found that the pressure drop penalty of

wavy microchannels can be much smaller than the heat transfer enhancement. The same conclusions have been obtained by Mohammed et al. [17] through a numerical study of the hydrothermal characteristics of wavy microchannel heat sink of rectangular cross-section with different wavy amplitudes ranged from 125 µm to 500 µm. The results showed that the thermal performance of wavy microchannel was more superior to that of straight microchannel. In the same time, they also found that the pressure drop penalty was much lower than the heat transfer enhancement. The study also revealed that the friction factor and shear stress in wavy microchannel increased proportionally with the waviness. In the same field but with different shapes, Gang et al. [18] have investigated numerically three-dimensional laminar fluid flow and heat transfer characteristics in two different types of wavy channels; serpentine channels and raccoon channels with rectangular cross-sectional of 500 µm hydraulic diameter. Three effects were studied; wavy feature amplitude, wavelength, and aspect ratio for different Reynolds numbers between 50 and 150. It was found that the wavy channels had provided an improvement up to 55% in the overall performance compared to straight microchannel. In addition, the researchers found that serpentine channels showed a better thermal performance than that of raccoon channels (convergent–divergent). Dai et al.[19] have conducted an experimental study of heat transfer and fluid flow in wavy microchannel. Two types of pathways were chosen to be studied; zigzag and sinusoidal with semi-circle cross-section (diameter 2mm). The study aimed to analyze the complex flow behavior in wavy microchannel using micro-PIV visualization and 3D reconstruction techniques. These techniques proved that the flow recirculation and the secondary flow which arose in the bends have a significant effect on heat transfer enhancement through disrupting the thermal boundary layer. The results also showed progress in the thermal performance of zigzag channel over sinusoidal channel.

Secondary flow is another technique that has been proven its effectiveness by many studies. According to Steinke and Kandlikar [15], secondary flow can be generated by creating small passages in the separating walls between the main channels or by incorporating offset strip fins. Colgan et al. [20] have conducted a practical study with an overall description of the design, fabrication, and testing of individual silicon microchannel. The study presented two designs for the channel's wall; staggered and continuous fins. The results showed that the staggered fins with 75 µm or 100 µm pitch were superior to continuous fin. Lee et al. [21] studied experimentally and numerically the heat transfer in MCHS by using oblique fins. The results revealed a high augmentation in heat transfer up to 103% for average Nusselt number and a reduction of maximum temperature rise by 12.6 °C. At the same time, it was found that the pressure drop was much lower than the heat transfer enhancement. In another study by the same researchers, a parametric analysis was conducted to find the optimal values for two design parameters; oblique fin pitch and oblique angle which gave the highest rate of secondary flow. The results showed that the effective angle was 27° and the fin pitch was 400 µm for a hydraulic diameter of 104 µm. In a separate numerical study, Kuppusamy et al. [22] introduced another design for the secondary channels in a form of oblique channel in alternating orientation. This new design showed an increase in thermal performance up to 146% and a reduction in thermal resistance and pressure drop to 76% and 6% respectively.

In the present study, the main concern is to investigate the effect combination of two heat transfer augmentation methods; channel curvature and secondary flows. A good research report was given by Bergles [23] and Singh et al. [24] for a single loop of branched wavy microchannel, however the research would have been more relevant if other significant parameters such as waviness of curvature, the width of secondary channel, and the angle of inclination had been explored. Therefore, this investigation searches to report the effects of

these parameters in order to find the optimal dimensions that can produce the best results. A three-dimensional numerical simulation is conducted to study the laminar convective heat transfer in wavy microchannel with secondary oblique channel of alternating orientation (WAOC). These channels are created in the separation wall between the channels with alternating orientation in the crest and trough zones to avoid fluid migration towards a particular channel. The results are compared to wavy microchannels without oblique secondary channel (WWOC) to find out the extent of heat transfer enhancement due to the addition of secondary channels.

2.0 NUMERICAL SIMULATION

Numerical simulation of a 3D conjugate heat transfer and fluid flow was performed in wavy microchannel heat sink with secondary flow in oblique channel of alternating orientation (WAOC) using finite volume based on the CFD software package FLUENT.

Figure 1 shows the wavy microchannel heat sink with alternating oblique secondary channels (WAOC). The computational domain consisted of a single wall which separates the two channels with one half-width of main channels on both sides as in Figure 1b and 1c. The flow direction in the channel is shown in Fig. 2.

The governing equations for the steady-state incompressible fluid flow for continuity, momentum, and energy are given as follows:

(a) Continuity equation

$$\nabla.(\overrightarrow{v}) = 0 \tag{1}$$

(b) Momentum equation

$$\nabla.(\rho\,\vec{v}\vec{v}) = \nabla P + \nabla.(\mu\nabla\vec{v}) \tag{2}$$

(c) Energy equations

$$\nabla.\left(\rho\vec{v}c_p T\right) = \nabla.(k\nabla T) \qquad (liquid) \tag{3}$$

$$\nabla.(k\nabla T) = 0 \qquad (solid) \tag{4}$$

The Nusselt number was calculated according to the following equation:

$$Nu = \frac{hD_h}{k_f} \tag{5}$$

where D_h, h, k_f are the hydraulic diameter, heat convection coefficient, and thermal conductivity respectively.

Penerbit Akademia Baru
Journal of Advanced Research in Fluid Mechanics and Thermal Sciences
ISSN (online): 2289-7879 | Vol. 25, No. 1. Pages 1-18, 2016

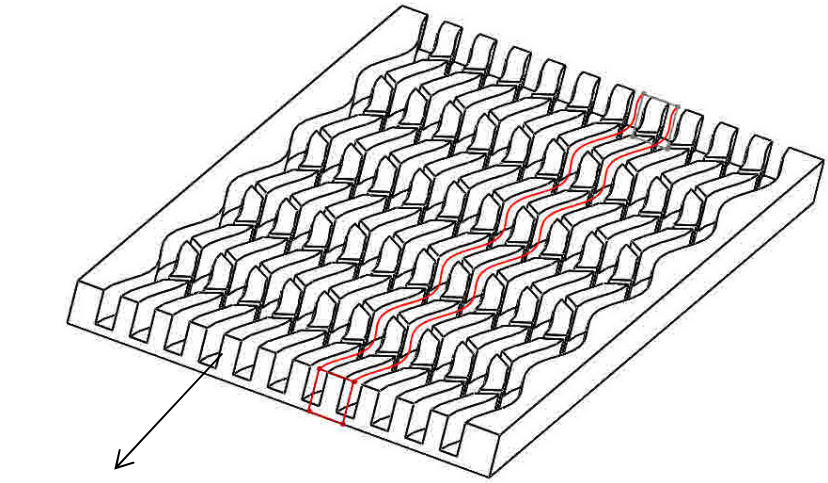

Computational domain

(a)

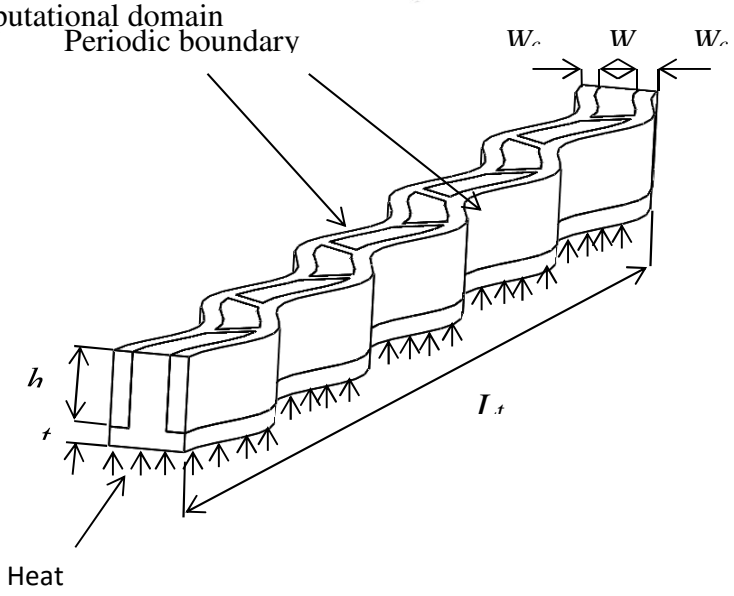

(b)

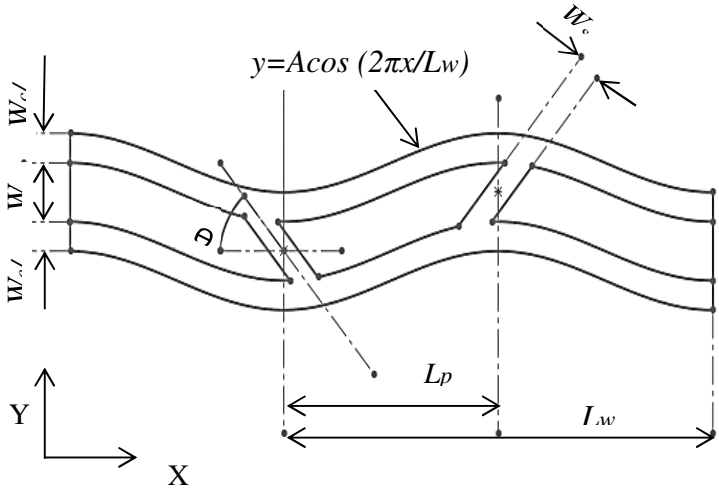

(c)

Figure 1: (a) A schematic diagram of WOAC; (b) a detailed view of the computational domain of WOAC; (c) dimensional details from top-view.

Penerbit Akademia Baru
Journal of Advanced Research in Fluid Mechanics and Thermal Sciences
ISSN (online): 2289-7879 | Vol. 25, No. 1. Pages 1-18, 2016

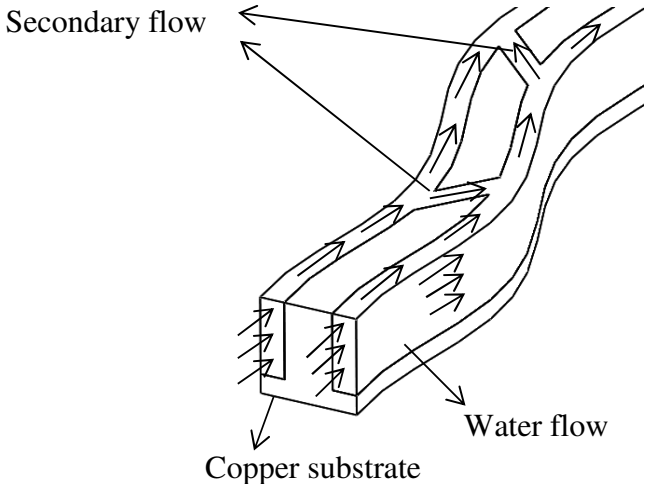

Figure 2: A schematic diagram of flow distributions in WOAC

The definition of Reynolds number is:

$$Re = \frac{\rho U D_h}{\mu} \tag{6}$$

where, μ is the fluid viscosity, ρ is the fluid density, and U is the average velocity.

The definition of hydraulic diameter is as follows:

$$D_h = \frac{4A}{P} = \frac{2W_C h_c}{(W_c + h_c)} \tag{7}$$

where A, P, W_C, h_c are the cross-sectional area, perimeter, channel width, and channel height respectively.

The friction factor was calculated based on the following equation:

$$f = \frac{\Delta P}{L} \times \frac{D_h}{2\rho u_m^2} \tag{8}$$

The heat transfer enhancement factor:

$$E_{Nu} = \frac{N_{u-WAOC}}{Nu-straight} \tag{9}$$

The pressure drop penalty factor:

$$E_P = \frac{\Delta P_{WAOC}}{\Delta P_{straight}} \tag{10}$$

A uniform heat flux of 500MW/m^2 was applied at the bottom of the surface of the copper substrate while all other surfaces were assumed adiabatic. Periodic boundary condition was applied at the outer surface on both sides of the computational domain as in Figure 1b. A

uniform velocity was specified at the inlet and outlet pressure. The working fluid was assumed as water with an inlet temperature of 300 K° and the substrate material was assumed as copper.

The computational domains were meshed with hexahedral volume elements using ANSYS ICEM-CFD. Three grid sizes were employed to check the mesh independence; 1 million, 1.2 million, and 1.5 million nodes. The results showed that the differences in pressure drop and Nusselt number between the solutions with the grids of 1.2 million and 1.5 million nodes were about 2.5% and 3% respectively. So, in order to save computational time and memory, the grid size of 1.2 million nodes was adopted in the present study.

Standard scheme was used for pressure discretization while SIMPLE scheme was used for velocity-pressure coupling. The momentum and energy equations were solved by using a second-order upwind scheme. The limits of residues for continuity and energy were considered to converge when they become less than 10^{-8} and 10^{-10} respectively.

To examine the validity of the numerical model, corroboration was made by solving the numerical model presented by Sui et al [25] and the results were compared with the present work. The model by Sui et al [25] consisted of a wavy microchannel with an amplitude of 0.05 mm, a channel height of 0.3 mm, and a channel width of 0.1 mm. Figure 3 shows the comparison between the current numerical model results and the results in a previous study [25] for heat transfer enhancement factor (ENu). The results showed a good agreement with an average error less than 1%.

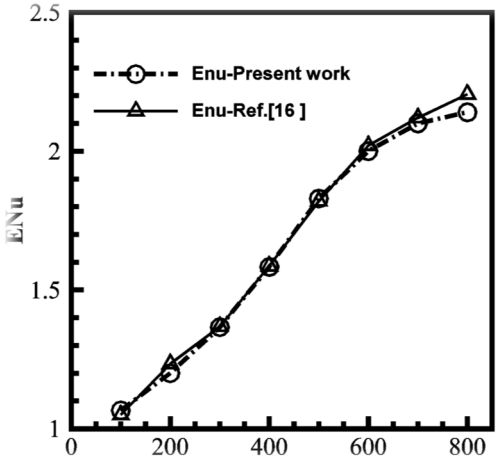

Figure 3: Validation of present work with ref [16]

3.0 RESULTS AND DISCUSSION

3.1 Effect of wave amplitude (A)

Figure 4 shows the impact of wavy amplitude and Reynolds number on the pressure drop penalty and heat transfer enhancement with respect to the straight channel. The heat transfer enhancement coefficient (E_{Nu}) and the pressure drop penalty coefficient (Ep) are defined as the average Nusselt and pressure drop of current WOAC divided by the corresponding values of straight channel [25].

Penerbit Akademia Baru
Journal of Advanced Research in Fluid Mechanics and Thermal Sciences
ISSN (online): 2289-7879 | Vol. 25, No. 1. Pages 1-18, 2016

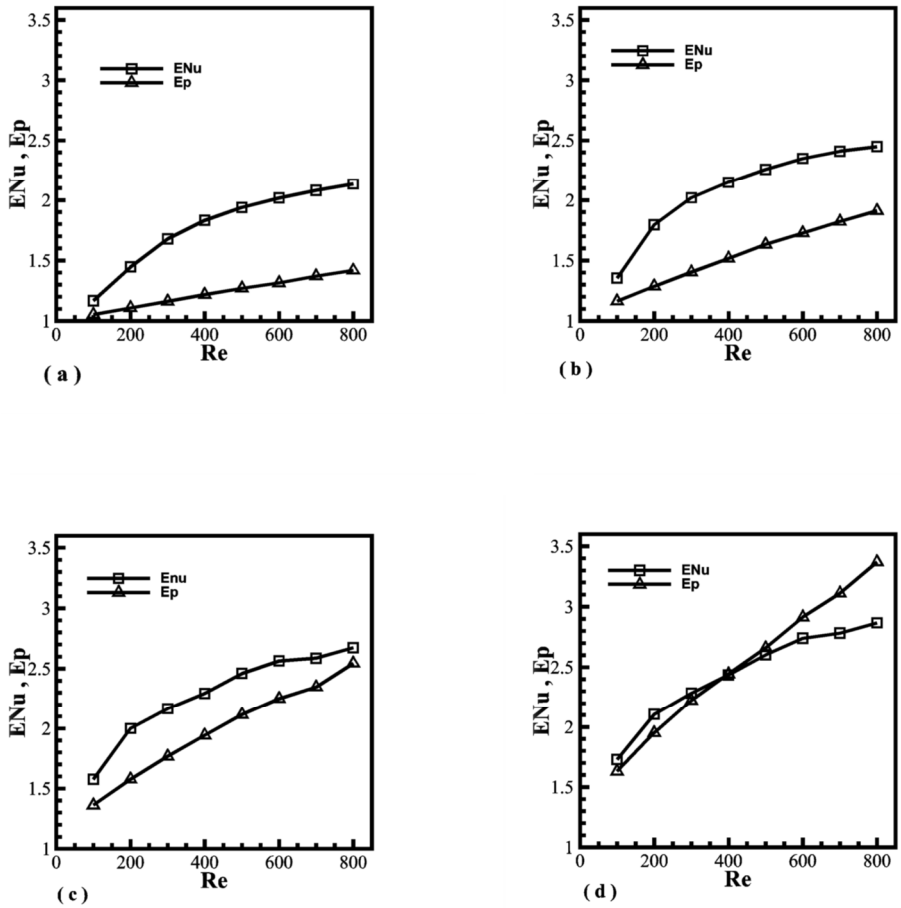

Figure 4: The variation of E_{Nu} and E_p with Reynolds number in (a) amplitude A=0.05mm, (b) A=0.1mm, (c) A=0.15mm, and (d) A=0.2mm

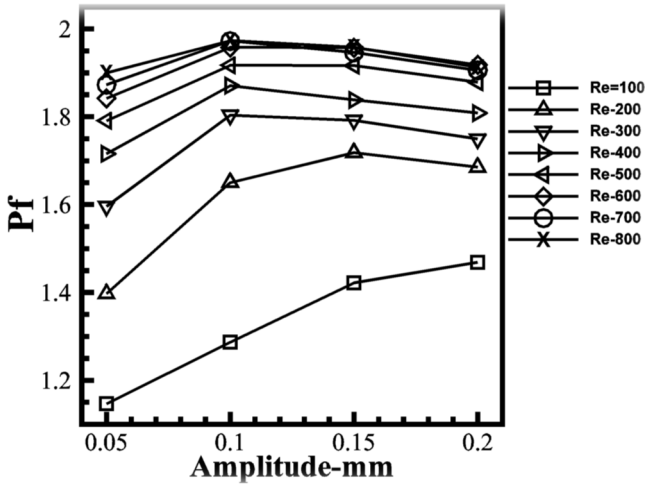

Figure 5: The variation of Pf with amplitudes

For all values of amplitudes from 0.05 to 0.2 mm as in Figure 4, it can be observed that both heat transfer enhancement coefficient (E_{Nu}) and pressure drop penalty coefficient (Ep) increased as the Reynolds number and amplitude (A) increased. The rate of increment varied according to the amplitude value. For small amplitudes, the increment in the heat transfer enhancement coefficient (E_{Nu}) was significantly larger than the increment in pressure drop penalty coefficient (Ep). For example, as shown in Figure 4a, at Re=800 and A=0.05, the E_{Nu} increased by about 113.5%, whereas the Ep increased by 41.8%. For larger amplitudes, the increment in pressure drop was more dominant than the increment in heat transfer. For example, as shown in Figure 4d, at Re=800 and A=0.2, the E_{Nu} increased by about 186% while Ep increased by 237%.

In order to determine the optimal amplitude that gives the best hydrothermal performance, a performance factor (Pf) was adopted as defined by Gong et al [18]. This factor is considered as an indicator to quantify the extent of enhancement in the overall performance of WAOC by making a comparison to the performance of the straight microchannel as in equation (11). Figure 5 demonstrates the tendency of (Pf) with Reynolds number for the range of amplitudes between 0.05 mm and 0.2 mm. In general, the performance factor increases parallel with the Reynolds number for all values of amplitude. In the range of low Reynolds number (100-200), it was found that the performance factor (Pf) increased considerably with high amplitude (such as in A=0.15, 0.2 mm). This increment reduced as the Reynolds number increased (Re>200) due to the negative effect of high-pressure drop. The optimal amplitude which achieved the highest performance was found at A=0.1 mm with Pf=2.

$$Pf = \frac{\frac{N_{u-WAOC}}{Nu-straight}}{\left(\frac{\Delta P_{WAOC}}{\Delta P_{straight}}\right)^{1/3}} = \frac{E_{Nu}}{Ep^{1/3}} \tag{11}$$

3.2 Effect of angle (θ)

The effect of the inclination angle of the secondary channel on each Nusselt number, pressure drop, and performance factor is discussed in this part. The angle was changed from 45° to 90° while the secondary channel width (Ws) and amplitude (A) were maintained at 0.1 mm.

As it is known in wavy channel, pressure increases significantly in the crest of the corrugated channel as a result of the centrifugal force of the fluid. The change of the secondary channel angle leads to the change of secondary channel orientation in which it become closer or far from the crest zone. In other words, when the angle (θ) increases, the secondary channel is oriented closer to the crest zone which means more pressure drop. Figure 6 shows that the pressure drop increased as the angle was increased to a maximum angle (90°).

The trend of Nusselt number is displayed in Figure 7 with the same range of angle and Reynolds number. The results showed a convergence in the Nusselt number values for all angles with a slight reduction at 90° with high Reynolds number (800-900) in spite of the occurrence of highest pressure drop at 90° which supposed to provide the highest rate of heat transfer. It is suggested that the increase in angle (θ) shifts the direction of the secondary channel towards the vertical axis which provides a shorter diagonal entry length at the diversion area of the fluid from the mainstream channel. This means the fluid volume and the contact surface area are reduced, hence lowered the rate of heat transfers.

Penerbit Akademia Baru
Journal of Advanced Research in Fluid Mechanics and Thermal Sciences
ISSN (online): 2289-7879 | Vol. 25, No. 1. Pages 1-18, 2016

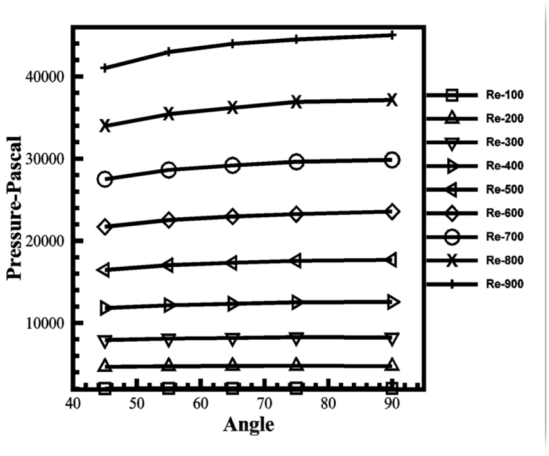

Figure 6: The variation of pressure drop with angle

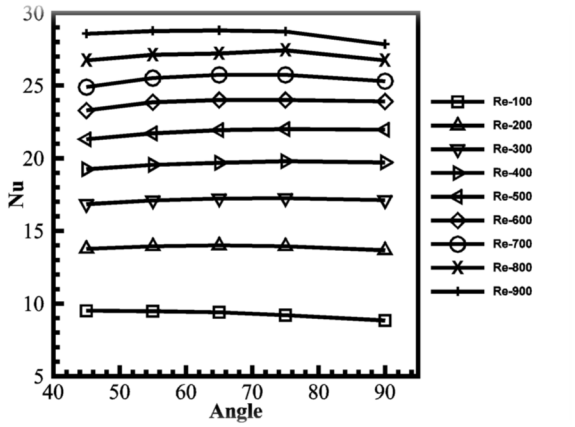

Figure 7: The variation of Nusselt number with angle

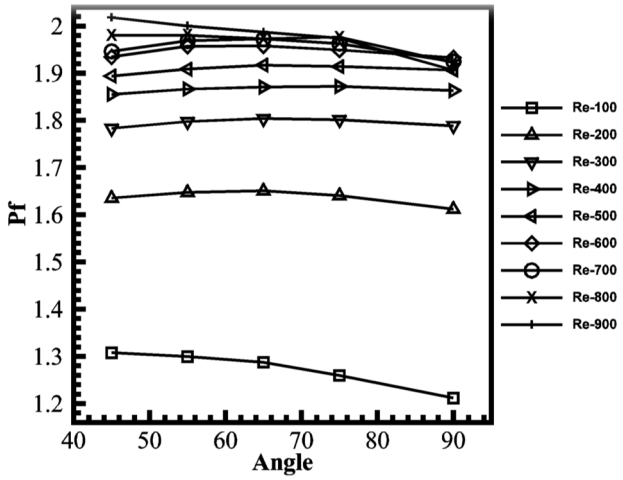

Figure 8: The variation of performance factor with angle

Penerbit Akademia Baru
Journal of Advanced Research in Fluid Mechanics and Thermal Sciences
ISSN (online): 2289-7879 | Vol. 25, No. 1. Pages 1-18, 2016

The results of Nusselt number and pressure drop were reflected in the trend of performance factor with the angle of secondary channel. Figure 8 shows that the angle 45° had achieved the highest performance factor (Pf), especially at high Reynolds number (800-900) because it possessed the lowest pressure drop. At the same time, the angle 90° had the lowest Pf because it possessed the highest pressure drop and the lowest Nusselt number.

3.3 Effect of width (W_s)

The effects of changing the secondary channel width (Ws) was studied according to the previous optimal results of amplitude and angle (A=0.1 mm, $\theta=45^0$). The width dimensions ranged between 0.1 mm and 0.2 mm, while the Reynolds number ranged from 100 to 900. Both the Nusselt number and pressure drop increased as the Reynolds number increased as shown in Figure 9 and Figure 10 respectively.

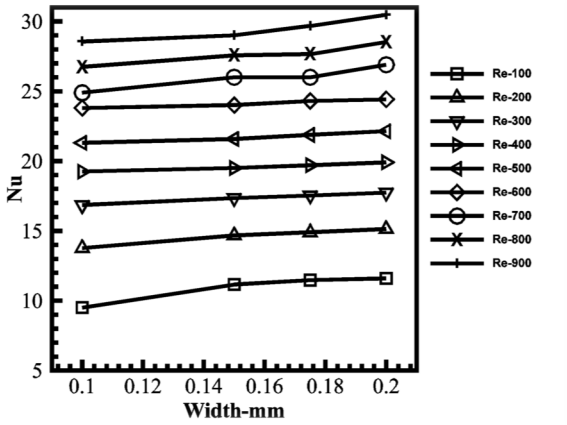

Figure 9: The variation of Nusselt number with width

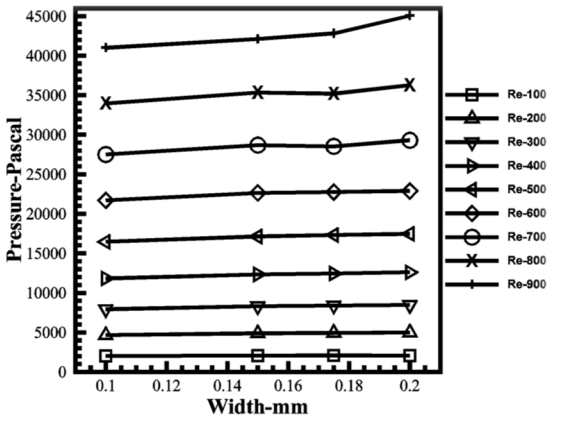

Figure 10: The variation of pressure drop with width

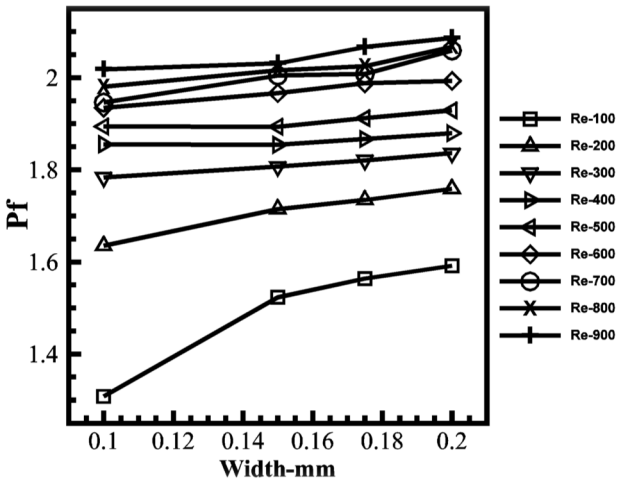

Figure 11: The variation of performance factor with width

With regards to the width increment, the results showed a slight increment in both Nusselt number and pressure drop which became more prominent in high Reynolds number (800-900). The performance factor showed a significant enhancement within the Reynolds number between 100 and 300 which was due to the low-pressure drop compared to the Nusselt number as in Figure 11. The width increment encourages a large volume of fluid to enter into the secondary channel, and thus increases the rate of heat exchange with inner surfaces. At the same time, the increment of the surface area causes more pressure drop due to the increment of friction between fluid and surfaces.

3.4 The overall comparison between WAOC and WWOC

A comparison study was conducted between WAOC and WWOC in order to recognize the extent of enhancement of hydro-thermal performance due to the existence of secondary channels. Figure 12 shows the trend of average Nusselt number with Reynolds number for both WAOC and WWOC. The average Nusselt number increased linearly with Reynolds number in both types with an appreciable superiority in WAOC. The maximum enhancement of average Nusselt number achieved in WAOC was about 28.5% more than that of WWOC.

On the other side, the pressure drop had witnessed an increase in WAOC more than WWOC for the same range of Reynolds number as in Figure 13. Both pressure curves were more converged at low Reynolds number (100-600) and diverged at high Reynolds number. Figure 14 also describes the trend of pressure drop along the centerline of axial direction for both channels at Re=800. This trend showed the pressure fluctuation in WAOC due to the presence of secondary channels. At the same time, the friction factor of WAOC was higher than WWOC as shown in Figure 15.

The current study also found that the performance factor of WAOC was superior to WWOC as shown in Figure 16. The extent of superiority at low Reynolds number was more than that of high Reynolds number because of the low-pressure drop.

Journal of Advanced Research in Fluid Mechanics and Thermal Sciences
ISSN (online): 2289-7879 | Vol. 25, No. 1. Pages 1-18, 2016

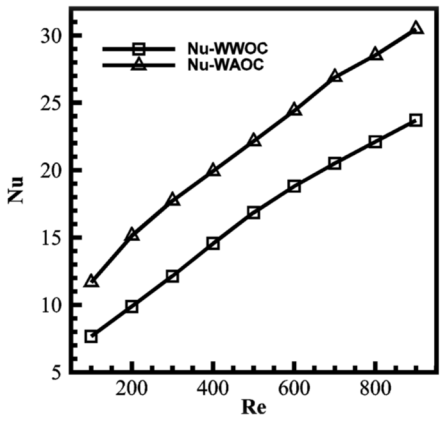

Figure 12: The variation of Nusselt number with Reynolds number for WAOC and WWOC

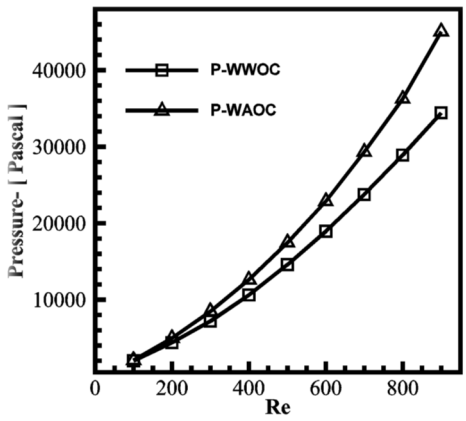

Figure 13: The variation of pressure drop with Reynolds number for WAOC and WWOC

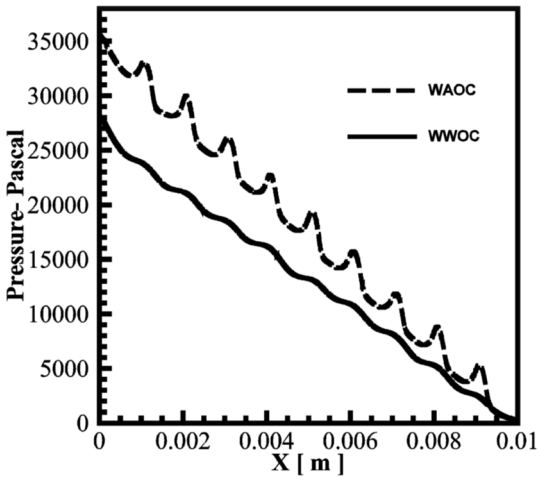

Figure 14: Pressure drop variation along the centerline of axial direction for both channels at Re=800

Penerbit Akademia Baru
Journal of Advanced Research in Fluid Mechanics and Thermal Sciences
ISSN (online): 2289-7879 | Vol. 25, No. 1. Pages 1-18, 2016

Figure 17 presents the temperature distribution along the centerline of the substrate base for both channels. This obviously showed the effect of secondary channel on temperature reduction in the substrate of WAOC.

Figure 18 displays the temperature contour in both channels at x-y plane with the same elevation (z=0.3mm). The temperature contour showed a reduction in the wall fin temperature of WAOC compared to WWOC due to the interruption and re-initialization in the boundary layers. In addition, the fluid diversion by secondary channels between the adjacent channels also increased the rate of heat exchange through the enhancement of fluid mixing as shown in the streamlines and velocity victor of WAOC in Figure 19b and Figure 20b respectively.

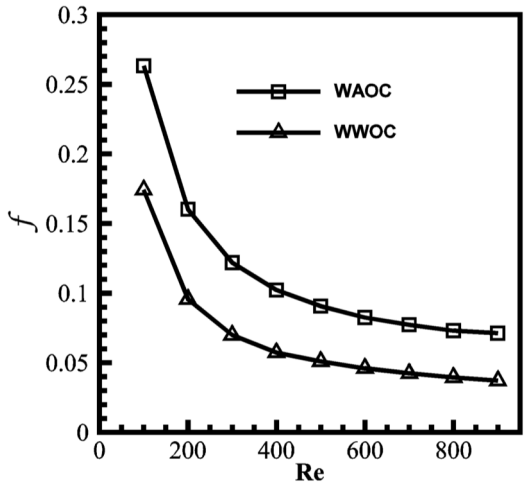

Figure 15: The variation of friction factor with Reynolds number for WAOC and WWOC

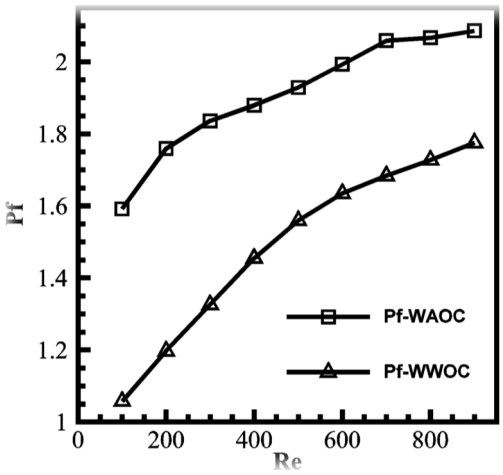

Figure 16: Variation of performance factor with Reynolds number for WAOC and WWOC

Penerbit Akademia Baru
Journal of Advanced Research in Fluid Mechanics and Thermal Sciences
ISSN (online): 2289-7879 | Vol. 25, No. 1. Pages 1-18, 2016

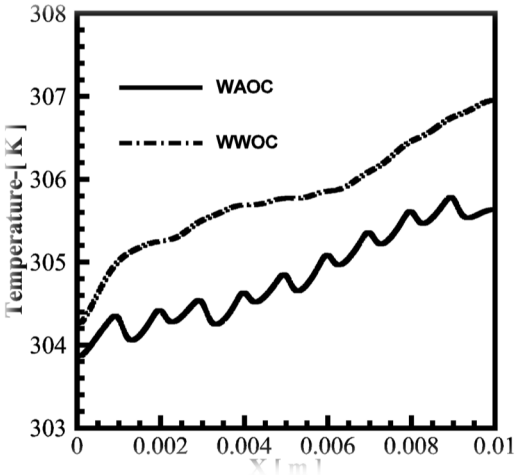

Figure 17: Variation of Temperature along the centerline of substrate base in the x-direction of WAOC and WWOC (Re=800)

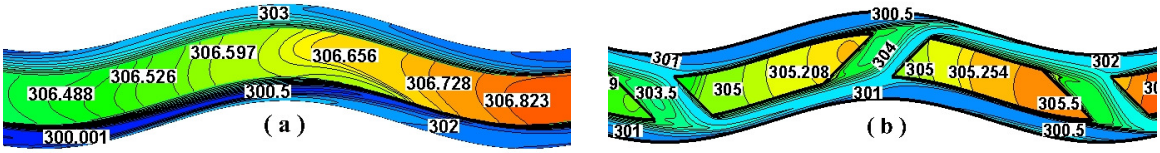

Figure 18. Temperature contour in x-y plane (x(4-6)mm) &elevation-z=0.3mm)-Re(600) in (a) WWOC and (b) WAOC

Figure 19: The streamlines in x-y plane (x(4-6)mm) & elevation-z=0.3mm)-Re(600) in (a) WWOC and (b) WAOC

Figure 20: The velocity vectors in x-y plane (x(4-6)mm) & elevation-z=0.3mm)-Re(600) in (a) WWOC and (b) WAOC

4.0 CONCLUSION

The hydrothermal performance of WAOC was numerically investigated to find the extent of heat transfer enhancement as the result of secondary channels insertion in a wavy microchannel. In addition, three structural parameters were studied; amplitude, secondary channel width, and its angle of inclination to find the optimum dimensions that will provide the best performance. The following are the conclusions of this study:

- The amplitude value showed a significant effect on the hydrothermal performance of WAOC in terms of pressure drop and Nusselt number. The high-pressure drop in high amplitude reduced the performance of WAOC in spite of the enhancement of Nusselt number.
- Changing the width of the secondary channel and its angle slightly affected the performance of WAOC in low and moderate range of Reynolds number but it showed a significant effect in high Reynolds number. This effect was illustrated by the enhanced performance with width increment and angle reduction.
- The performance of WAOC was superior to straight microchannel by 108%.
- The Nusselt number of the WAOC was superior to WWOC by 28.5%.

The WAOC can achieve the same heat transfer rate as in WWOC with a reduction in pressure drop up to 60%.

REFERENCES

[1] Association, S.I. "International Technology Roadmap for Semiconductors (Itrs), 2003 Edition." Hsinchu, Taiwan, Dec (2003).

[2] Tuckerman, D.B., and R. Pease. "High-Performance Heat Sinking for Vlsi." Electron Device Letters, IEEE 2, no. 5 (1981): 126-29.

[3] Razali, A. A., and A. Sadikin. "CFD Simulation Study on Pressure Drop and Velocity across Single Flow Microchannel Heat Sink." Journal of Advanced Research Design 8, no. 1 (2015): 12-21.

[4] Rahman, M.M., and F. Gui. "Experimental Measurements of Fluid Flow and Heat Transfer in Microchannel Cooling Passages in a Chip Substrate." Paper presented at the The ASME International Electronics Packaging Conference, Binghamton, NY, USA, 09/29-10/02/93, 1993.

[5] Noh, NH Mohamad, A. Fazeli, and NA Che Sidik. "Numerical Simulation of Nanofluids for Cooling Efficiency in Microchannel Heat Sink." J Adv Res Fluid Mech Therm Sci 4 (2014): 13-23.

[6] Lee, P.-S., S.V. Garimella, and D. Liu. "Investigation of Heat Transfer in Rectangular Microchannels." International Journal of Heat and Mass Transfer 48, no. 9 (2005): 1688-704.

[7] Owhaib, W., and B. Palm. "Experimental Investigation of Single-Phase Convective Heat Transfer in Circular Microchannels." Experimental Thermal and Fluid Science 28, no. 2 (2004): 105-10.

[8] Abubakar, S.B., N. A. Che Sidik and A.S. Ahmad. "The use of Fe_3O_4-H_2O_4 Nanofluid for Heat Transfer Enhancement in Rectangular Microchannel Heatsink." Journal of Advanced Research in Materials Science 23, no. 1 (2016): 15-24.

[9] Chen, Y., C. Zhang, M. Shi, and J. Wu. "Three-Dimensional Numerical Simulation of Heat and Fluid Flow in Noncircular Microchannel Heat Sinks." International Communications in Heat and Mass Transfer 36, no. 9 (2009): 917-20.

[10] Abubakar, S. B., and NA Che Sidik. "Numerical Prediction of Laminar Nanofluid Flow in Rectangular Microchannel Heat Sink." J Adv Res Fluid Mech Therm Sci 7 (2015): 29-38.

[11] Mohammed, H., P. Gunnasegaran, and N. Shuaib. "The Impact of Various Nanofluid Types on Triangular Microchannels Heat Sink Cooling Performance." International Communications in Heat and Mass Transfer 38, no. 6 (2011): 767-73.

[12] Agarwal, A., T.M. Bandhauer, and S. Garimella. "Measurement and Modeling of Condensation Heat Transfer in Non-Circular Microchannels." international journal of refrigeration 33, no. 6 (2010): 1169-79.

[13] Alfaryjat, A., H. Mohammed, N.M. Adam, M. Ariffin, and M. Najafabadi. "Influence of Geometrical Parameters of Hexagonal, Circular, and Rhombus Microchannel Heat Sinks on the Thermohydraulic Characteristics." International Communications in Heat and Mass Transfer (2014).

[14] Gunnasegaran, P., H. Mohammed, N. Shuaib, and R. Saidur. "The Effect of Geometrical Parameters on Heat Transfer Characteristics of Microchannels Heat Sink with Different Shapes." International Communications in Heat and Mass Transfer 37, no. 8 (2010): 1078-86.

[15] Steinke, M.E., and S.G. Kandlikar. "Review of Single-Phase Heat Transfer Enhancement Techniques for Application in Microchannels, Minichannels and Microdevices." International Journal of Heat and Technology 22, no. 2 (2004): 3-11.

[16] Sui, Y., P. Lee, and C. Teo. "An Experimental Study of Flow Friction and Heat Transfer in Wavy Microchannels with Rectangular Cross Section." International Journal of Thermal Sciences 50, no. 12 (2011): 2473-82.

[17] Mohammed, H., P. Gunnasegaran, and N. Shuaib. "Numerical Simulation of Heat Transfer Enhancement in Wavy Microchannel Heat Sink." International Communications in Heat and Mass Transfer 38, no. 1 (2011): 63-68.

[18] Gong, L., K. Kota, W. Tao, and Y. Joshi. "Parametric Numerical Study of Flow and Heat Transfer in Microchannels with Wavy Walls." Journal of Heat Transfer 133, no. 5 (2011): 051702.

[19] Dai, Z., D.F. Fletcher, and B.S. Haynes. "Impact of Tortuous Geometry on Laminar Flow Heat Transfer in Microchannels." International Journal of Heat and Mass Transfer 83 (2015): 382-98.

[20] Colgan, E.G., B. Furman, M. Gaynes, W.S. Graham, N.C. LaBianca, J.H. Magerlein, R.J. Polastre, M.B. Rothwell, R. Bezama, and R. Choudhary. "A Practical Implementation of Silicon Microchannel Coolers for High Power Chips." Components and Packaging Technologies, IEEE Transactions on 30, no. 2 (2007): 218-25.

[21] Lee, Y., P. Lee, and S. Chou. "Enhanced Thermal Transport in Microchannel Using Oblique Fins." Journal of Heat Transfer 134, no. 10 (2012): 101901.

[22] Raja Kuppusamy, N., R. Saidur, N.N.N. Ghazali, and H.A. Mohammed. "Numerical Study of Thermal Enhancement in Micro Channel Heat Sink with Secondary Flow." International Journal of Heat and Mass Transfer 78, no. 0 (2014): 216-23.

[23] Bergles, A.E. "Exhft for Fourth Generation Heat Transfer Technology." Experimental Thermal and Fluid Science 26, no. 2–4 (2002): 335-44.

[24] Singh, P.K., H.F.S. Tan, C.J. Teo, and P.S. Lee. "Flow and Heat Transfer in Branched Wavy Microchannels." Paper presented at the ASME 2013 4th International Conference on Micro/Nanoscale Heat and Mass Transfer, 2013.

[25] Sui, Y., C. Teo, P. Lee, Y. Chew, and C. Shu. "Fluid Flow and Heat Transfer in Wavy Microchannels." International Journal of Heat and Mass Transfer 53, no. 13 (2010): 2760-72.